

Nonlinear Optics

Observation of Discrete Vortex Solitons in 2D Photonic Lattices

Jason W. Fleischer, Dragomir N. Neshev, Guy Bartal, Tristram J. Alexander, Oren Cohen, Elena A. Ostrovskaya, Ofer Manela, Hector Martin, Jared Hudock, Igor Makasyuk, Zhigang Chen, Demetrios N. Christodoulides, Yuri S. Kivshar and Mordechai Segev

Vortex dynamics in nonlinear arrays remains an outstanding problem in lattice physics. Angular momentum is fundamental to dynamics in two dimensions (2D), while discretization effects and Bragg reflections impose severe constraints on wave propagation. Indeed, nonlinear lattices can support self-localized states that cannot exist in homogeneous media, e.g., vortex-ring solitons. Despite their importance to a variety of fields ranging from biology to photonics to matter waves in Bose-Einstein condensates, such discrete vortex solitons have not been studied until recently.^{1,2} Moreover, the relatively new ability to create nonlinear waveguide arrays in two dimensions³⁻⁵ has allowed them to be observed experimentally.^{6,7}

Here, we summarize the independent observations of vortex-ring lattice solitons by two separate groups. Both relied on optical induction to create a nonlinear lattice in a photosensitive (photorefractive) material.³ In this technique, shown schematically in the figure, ordinarily polarized light is periodically modulated (by interference or by imaging a mask) to induce a 2D array of waveguides in an anisotropic photorefractive crystal. A separate probe beam of extraordinary polarization acquires a vortex structure by passing through a phase mask and is then launched into the array. The degree of nonlinearity is controlled by applying a voltage across the *c*-axis of the crystal (photorefractive screening nonlinearity) and controlling the intensity of the probe beam.

There are several types of vortex lattice solitons, but the most fundamental (single-charge) ones are the on-site vortex, in which the singularity is located on a waveguide channel, and the off-site vortex, in which the singularity is between sites. In

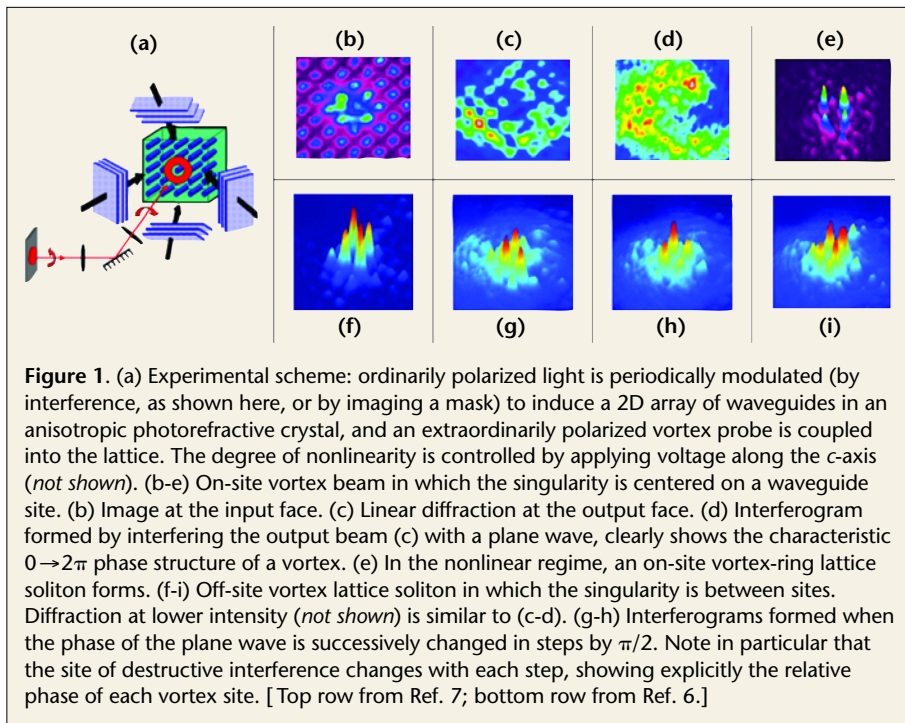


Figure 1. (a) Experimental scheme: ordinarily polarized light is periodically modulated (by interference, as shown here, or by imaging a mask) to induce a 2D array of waveguides in an anisotropic photorefractive crystal, and an extraordinarily polarized vortex probe is coupled into the lattice. The degree of nonlinearity is controlled by applying voltage along the *c*-axis (*not shown*). (b-e) On-site vortex beam in which the singularity is centered on a waveguide site. (b) Image at the input face. (c) Linear diffraction at the output face. (d) Interferogram formed by interfering the output beam (c) with a plane wave, clearly shows the characteristic $0 \rightarrow 2\pi$ phase structure of a vortex. (e) In the nonlinear regime, an on-site vortex-ring lattice soliton forms. (f-i) Off-site vortex lattice soliton in which the singularity is between sites. Diffraction at lower intensity (*not shown*) is similar to (c-d). (g-h) Interferograms formed when the phase of the plane wave is successively changed in steps by $\pi/2$. Note in particular that the site of destructive interference changes with each step, showing explicitly the relative phase of each vortex site. [Top row from Ref. 7; bottom row from Ref. 6.]

contrast with the 1D analogues of Sievers-Takeno and Page modes, respectively, both of the basic types are stable.^{1,2} Experimentally, both the on-site⁷ and off-site^{6,7} vortex lattice solitons have been observed.

Typical results for an on-axis vortex beam are shown in the figure. At low intensity, the vortex beam simply diffracts across the crystal. An interferogram, formed by interfering the output with a plane wave, clearly shows the $0 \rightarrow 2\pi$ phase structure of the vortex. In the nonlinear regime, self-focusing creates a steady-state soliton that keeps its profile. In the corresponding interferogram, changing the phase of the reference plane wave changes the site of destructive interference, proving that the lattice soliton keeps its vortex phase structure. This is a nontrivial result, since lattices break the continuous rotational symmetry of homogeneous media and do not generally conserve angular momentum (topological charge). In this case, a combination of “discrete” dynamics and nonlinearity allows the soliton to maintain its vortex phase. Note that it is also this combination that allows a stable ring structure, since bright rings (with or without topological charge) are unstable in homogeneous media with self-focusing nonlinearity.

In conclusion, both on-site and off-site vortex lattice solitons have been experimentally observed in nonlinear waveguide arrays. These vortex-ring solitons are generic to nonlinear lattices in two dimensions and are building blocks for more extended and complex wave structures. We anticipate that the dynamics observed here will appear in the near future in other systems, such as nonlinear fiber bundles, photonic crystal fibers and Bose-Einstein condensates.

Jason W. Fleischer, Guy Bartal, Oren Cohen, Ofer Manela and Mordechai Segev are with the Dept. of Physics, Technion-Israel Institute of Technology, Haifa. Fleischer was also with the School of Optics/CREOL, University of Central Florida, Orlando. He is now at Princeton University. Jared Hudock and Demetrios N. Christodoulides are with the School of Optics/CREOL. Dragomir N. Neshev, Tristram J. Alexander, Elena A. Ostrovskaya and Yuri S. Kivshar are with the Nonlinear Physics Centre, Research School of Physical Sciences and Engineering, Australian National University, Canberra. Hector Martin, Igor Makasyuk and Zhigang Chen are with the Dept. of Physics and Astronomy, San Francisco State University, Calif. Zhigang Chen is also with TEDA College, Nankai University, Tianjin, China.

References

1. B. A. Malomed and P.G. Kevrekidis, *Phys. Rev. E* **64**, 026601 (2001).
2. J. Yang and Z.H. Musslimani, *Opt. Lett.* **28**, 2094 (2003).
3. N. K. Efremidis et al., *Phys. Rev. E* **66**, 046602 (2002).
4. J. W. Fleischer et al., *Nature* **422**, 147 (2003).
5. H. Martin et al., *Phys. Rev. Lett.* **92**, 123902 (2004).
6. D. N. Neshev et al., *Phys. Rev. Lett.* **92**, 123903 (2004).
7. J. W. Fleischer et al., *Phys. Rev. Lett.* **92**, 123904 (2004).

Observation of Discrete Modulational Instability

J. Meier, G. I. Stegeman, D. N. Christodoulides, Y. Silberberg, R. Morandotti, H. Yang, G. Salamo, M. Sorel and J. S. Aitchison

Nonlinear periodic lattices are known to exhibit unique properties that find no analogue whatsoever in homogeneous systems. For example, the diffraction (beam spreading) properties of arrays of coupled channel waveguides can exhibit either normal or anomalous spatial diffraction, depending on the direction of propagation. In the case of high intensity waves, changes in the diffraction relation have a significant impact on their stability. In bulk materials with positive nonlinearity, a high intensity beam will either form a bright spatial soliton or will break up due to modulational instability (MI). In a totally analogous fashion, a broad optical beam propagating in a self-focusing nonlinear array will experience discrete MI and filamentation, provided that its transverse wave vector lies within the region of normal diffraction.² In contrast, in the anomalous diffraction region of this same system, a high power optical beam will be stable as a direct result of discreteness.³ This is similar to the case of pulse propagation in glass fibers, where MI and filamentation are only possible in the anomalous group velocity dispersion regime, not in the normal regime.⁴

In a recent experimental study,⁵ we were able to demonstrate, for the first time to our knowledge, the spatial stability properties of waves in a discrete optical system. We used arrays consisting of 101 AlGaAs waveguides to propagate wide, high power beams from a picosecond optical parametric amplifier and observed the output intensity distribution for different powers and propagation angles. For the experiment, in order to minimize nonlinear absorption effects, we chose a wavelength of 1,550 nm (less than half the bandgap energy of AlGaAs). In Fig. 1, we show the recorded intensity distribution at the output facet of the AlGaAs array for different powers and for variations in the angle of incidence of the beam. The angle of incidence is related to the phase difference between neighboring waveguides Q which in turn determines

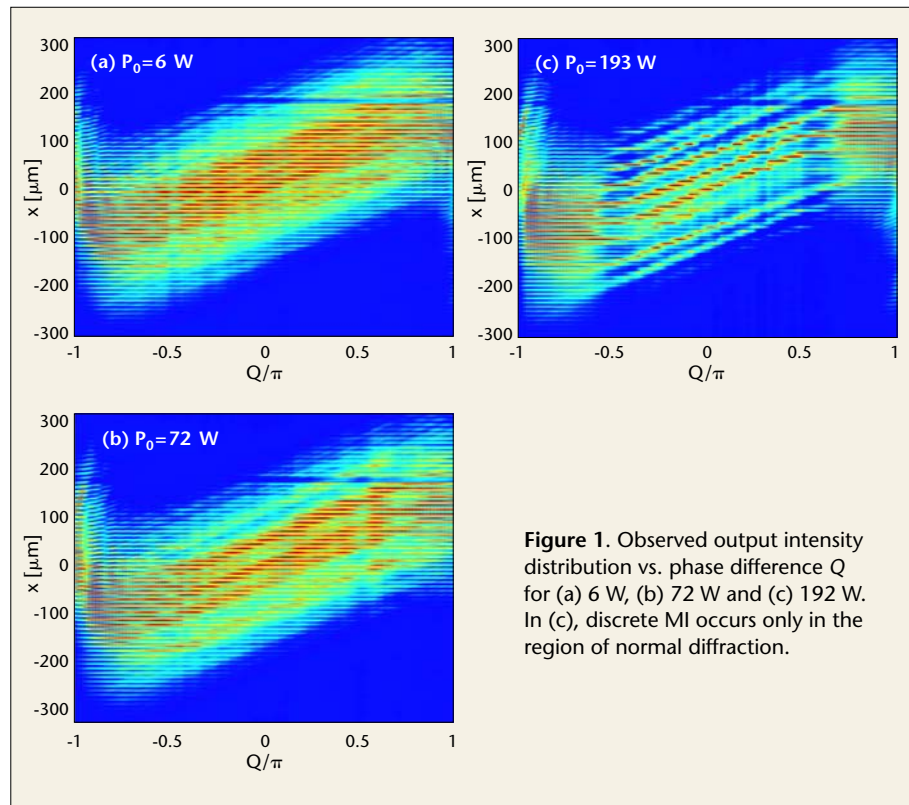


Figure 1. Observed output intensity distribution vs. phase difference Q for (a) 6 W, (b) 72 W and (c) 192 W. In (c), discrete MI occurs only in the region of normal diffraction.

the dispersion properties of the array. For a phase difference of between $\pm\pi/2$, the array exhibits normal diffraction, whereas for $\pi/2 < |Q| < \pi$, the diffraction of the array is anomalous. At low peak powers (6 W in the central waveguide), the only noise observable at the output is due to distortions of the input beam and imperfections in the sample. An increase to 72 W of the input power gives rise to the growth of the noise from these sources because of discrete MI in the normal diffraction region, while in the anomalous diffraction regime no such growth is observable. At 193 W, the highest input power level shown, we observe the breakup of the beam into discrete filaments which are highly localized in a few channels. Previous observations of highly localized discrete solitons showed that the power needed to excite what was essentially a “single channel” soliton in these samples was of the order of 1–2 kW. To form this type of discrete soliton train, each MI filament collects power from neighboring channels. However, in the anomalous diffraction region, the beam maintains its original shape, even when excited with 193 W per waveguide.

In conclusion, we have reported what is to our knowledge the first experimental observation of MI in a discrete optical system. The experimental results agree well with theoretical predictions. This phenomenon is expected to be universal to all discrete systems.

Acknowledgment

This work was supported in part by an ARO MURI.

J. Meier, G. I. Stegeman and D. N. Christodoulides are with the College of Optics and Photonics–CREOL & FPCE, University of Central Florida, Orlando, Fla. Y. Silberberg is with the Department of Physics of Complex Systems, the Weizmann Institute of Science, Rehovot, Israel. R. Morandotti is with the Institut National de la Recherche Scientifique, Université du Québec, Varennes, Québec, Canada. H. Yang and G. Salamo are with the Physics Department, University of Arkansas, Fayetteville, Ark. M. Sorel is with the Department of Electrical and Electronic Engineering, University of Glasgow, Scotland. J. S. Aitchison is with the Department of Electrical and Computer Engineering, University of Toronto, Ontario, Canada.

References

1. H. S. Eisenberg et al., *Phys. Rev. Lett.*, **85**, 1863 (2000).
2. D. N. Christodoulides and R. I. Joseph, *Opt. Lett.*, **13**, 794 (1988).
3. Y. S. Kivshar and M. Peyrard, *Phys. Rev. A* **46**, 3198 (1992).
4. G. P. Agrawal, *Nonlinear Fiber Optics*, (Academic Press, Boston, 1989).
5. J. Meier et al., *Phys. Rev. Lett.* **92**, 163902 (2004).

Large Kerr Nonlinearity at Low Light Intensities

Hoonsoo Kang and Yifu Zhu

Kerr nonlinearity represents the dispersive part of third-order susceptibilities in an optical medium and has found many applications in nonlinear optics. Recent studies have shown that Kerr nonlinearity can be used for quantum nondemolition measurements, quantum logic gates and quantum state teleportation. For such applications, it is desirable to have large Kerr nonlinearity with high sensitivities at low light intensities. This requires that, for all pump and signal fields, the linear susceptibility should be as small as possible so as to minimize absorption loss. In conventional devices, however, these requirements are incompatible. To overcome this difficulty, Schmidt and Imamoglu proposed a scheme based on a four-level system with electromagnetically induced transparency (EIT).¹ The EIT scheme is capable of producing greatly enhanced third-order susceptibilities while at the same time completely suppressing linear susceptibilities. The corresponding Kerr nonlinearity can be many orders of magnitude greater than that obtained in a conventional three-level scheme and can be used to obtain large cross-phase modulation (XPM) at weak light intensities. The absorptive part of the enhanced third-order nonlinearities can be used to realize a quantum switch operating at single photon levels.²⁻⁴

The four-level EIT system which exhibits greatly enhanced Kerr nonlinearity is depicted in Fig. 1(a).² A coupling laser driving the transition $|2\rangle \rightarrow |3\rangle$ with Rabi frequency Ω_c and a probe laser driving the transition $|1\rangle \rightarrow |3\rangle$ with Rabi frequency Ω_p create the standard Λ -type EIT. A signal laser drives the transition $|2\rangle \rightarrow |4\rangle$ with Rabi frequency Ω and induces XPM on the probe laser. In the dressed-state picture [Fig. 1(b)], the signal laser induces cross-phase modulation of the probe laser similar to that in the conventional three-level XPM scheme. Because the linear absorption and dispersion of the probe laser are suppressed by EIT, the Kerr nonlinearity is resonantly enhanced and the resulting XPM can

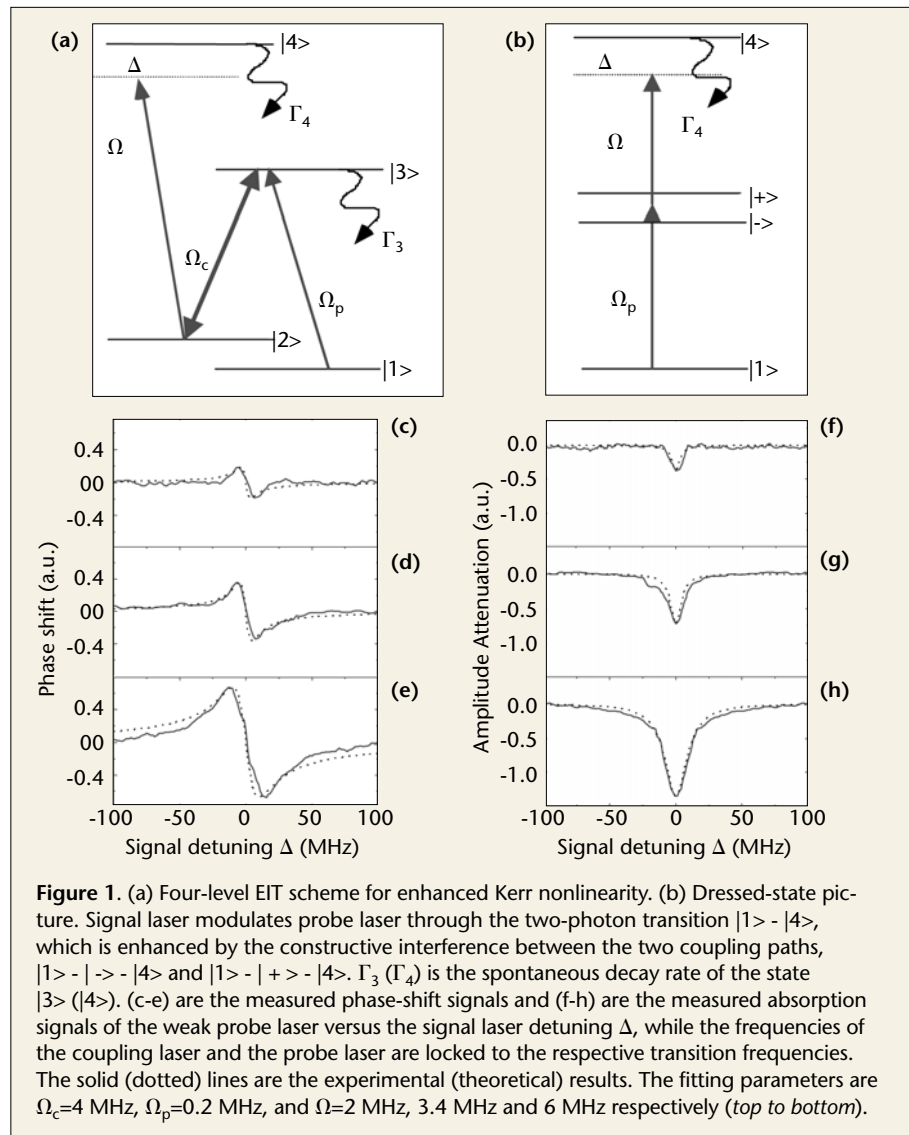


Figure 1. (a) Four-level EIT scheme for enhanced Kerr nonlinearity. (b) Dressed-state picture. Signal laser modulates probe laser through the two-photon transition $|1\rangle \rightarrow |4\rangle$, which is enhanced by the constructive interference between the two coupling paths, $|1\rangle \rightarrow |-\rangle \rightarrow |4\rangle$ and $|1\rangle \rightarrow |+\rangle \rightarrow |4\rangle$. Γ_3 (Γ_4) is the spontaneous decay rate of the state $|3\rangle$ ($|4\rangle$). (c-e) are the measured phase-shift signals and (f-h) are the measured absorption signals of the weak probe laser versus the signal laser detuning Δ , while the frequencies of the coupling laser and the probe laser are locked to the respective transition frequencies. The solid (dotted) lines are the experimental (theoretical) results. The fitting parameters are $\Omega_c=4$ MHz, $\Omega_p=0.2$ MHz, and $\Omega=2$ MHz, 3.4 MHz and 6 MHz respectively (top to bottom).

be observed under very low signal laser intensities.

We observed large Kerr nonlinearity in the four-level EIT scheme and the resulting large XPM in cold Rb atoms confined in a magneto-optical trap (MOT).⁵ The frequency modulation technique was employed to measure both the probe laser phase shift and the amplitude attenuation.

The measurement results are presented in Fig. 1(c-h). The peak nonlinear absorption coefficient is ~ 0.5 [Fig. 1(h)] and the peak XPM phase shift is ~ 8 degrees [Fig. 1(e)]. The measured XPM shifts [Fig. 1(c-e)] are more than three orders of magnitude greater than that of the conventional three-level Kerr nonlinearity under similar conditions.

The EIT scheme for producing large Kerr nonlinearity has attracted considerable attention because of its potential applications in quantum optics, nonlinear optics and quantum information science. Recently, for example, quantum teleportation and quantum logic gates based on EIT enhanced Kerr nonlinearities have been proposed.

Hoonsoo Kang and Yifu Zhu (yifuzhu@fiu.edu) are with the Department of Physics, Florida International University, Miami.

References

1. H. Schmidt and A. Imamoglu, *Opt. Lett.* **21**, 1936 (1996).
2. S. E. Harris and Y. Yamamoto, *Phys. Rev. Lett.* **81**, 3611 (1998).
3. M. Yan et al., *Opt. Lett.* **26**, 548-50 (2001).
4. D. A. Braje, et al., *Phys. Rev. A* **68**, 041801(R) (2003).
5. H. Kang and Y. Zhu, *Phys. Rev. Lett.* **91**, 93601 (2003).